Comparative studies on field emission properties of carbon-based materials

K.H. Chen [a],[*], J.-J. Wu [a], L.C. Chen [b], C.Y. Wen [b], P.D. Kichambare [b], F.G. Tarntair [c], P.F. Kuo [d], S.W. Chang [d], Y.F. Chen [d]

[a] *Institute of Atomic and Molecular Sciences, Academia Sinica, Taipei, Taiwan*
[b] *Center for Condensed Matter Sciences, National Taiwan University, Taipei, Taiwan*
[c] *Department of Electronic Engineering, National Chiao Tung University, Hsinchu, Taiwan*
[d] *Department of Physics, National Taiwan University, Taipei, Taiwan*

Abstract

Comparative studies on field emission properties of various carbon-related materials including diamond, amorphous carbon, SiCN films, SiCN nanorods, and carbon nanotubes are presented. While diamond is well known for its potential use in cold cathodes, the emission current of a hydrogen-treated diamond film is relatively small compared to that of amorphous carbon or diamond-like-carbon film. Meanwhile, carbon nanotubes have demonstrated large emission currents at much lower threshold voltages, showing their potential for applications. However, the emission from carbon nanotubes is subjected to significant decay under long-term operation. The emission current and long-term stability can be improved using a new SiCN compound with nanorod morphology. The effective barrier height and the field enhancement factor derived from the Fowler–Nordheim equation are discussed in this paper. © 2000 Elsevier Science S.A. All rights reserved.

Keywords: Amorphous carbon; Carbon-based materials; Carbon nanotubes; Diamond; Field emission properties; SiCN films; SiCN nanorods

1. Introduction

In the past few years, considerable interest has been focused on the electron field emission from diamond and related materials [1–3]. Due to its negative electron affinity property, diamond has been widely recognized as the dream material for various applications from cold cathodes, flat panel displays, to a new generation of microwave tubes. Experimental data, however, indicate that non-diamond phases such as diamond-like carbon (DLC), amorphous carbon (a-C), and other nanostructural carbon demonstrate a much better field-emission property than that of diamond [4,5]. The addition of dopants into the material can substantially reduce the onset field from 30 V/μm typically to a few V/μm, and can enhance the emission current up to hundreds of μA/cm [2,6]. It has been demonstrated that the introduction of an sp^2 phase in the film further reduces the onset field intensity and enhances the emission current [7].

With the advent of nanometer materials such as carbon nanotubes, the carbon-based electron field emitter experienced another rush, bringing the idea of cold-cathode closer to reality.

In this report, a comparison of materials produced in our laboratory ranging from bias-assisted carburized (BAC) silicon tips [8], SiCN nano-crystallite [9,10], SiCN nanorods [11], and carbon nanotubes [12] is made to elucidate the mechanisms of field emission. The correlations of the material, the field enhancement factor (geometry of the sample) and the effective barrier height (work function) to the emission current are investigated.

2. Experimental

2.1. Sample preparation

A silicon microtip array (50×50 square and 1 μm in width) of each tip was produced by standard photolithography and reactive ion etching processes. The ultra-high aspect ratio cone-shaped microtip array was

* Corresponding author. Fax: +886-2-2362-0200.
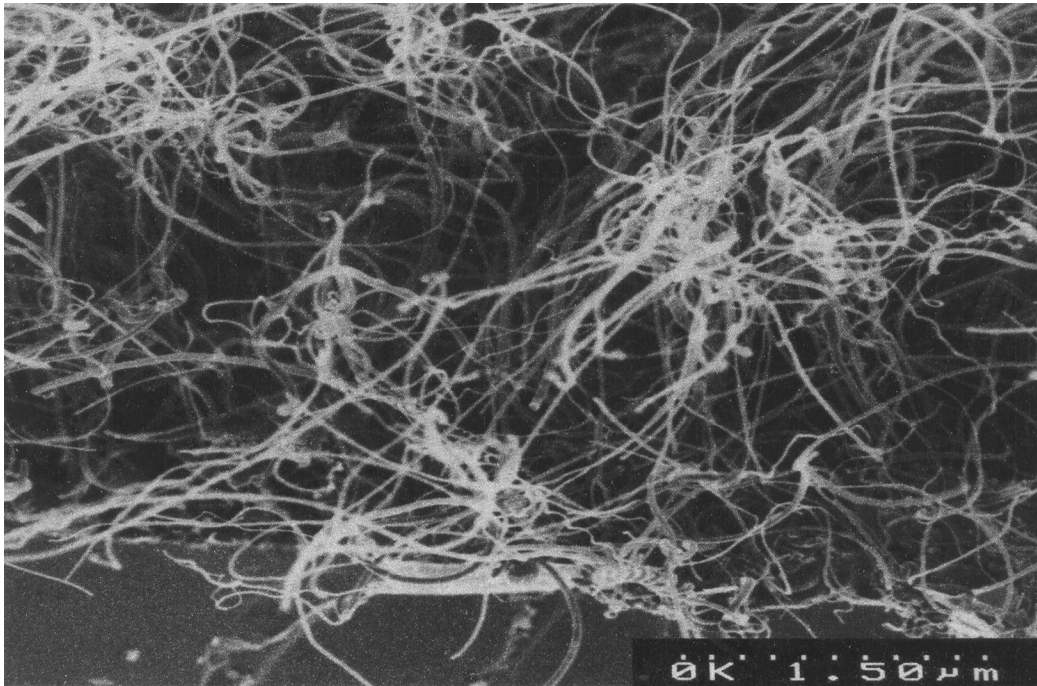*E-mail address:* chenkh@po.iams.sinica.edu.tw (K.H. Chen)

Fig. 1. Typical SEM micrograph of carbon nanotubes.

further coated with a carbon layer using the BAC process. Selective deposition of the carbon layer on the surface of sharp silicon tips was achieved by careful adjustment of the bias voltage and bias time. The optimal conditions for the BAC were -200 V bias voltage for 40 min with 25% CH_4 in H_2 using a microwave plasma CVD reactor at a substrate temperature of 650°C. Typically, sharp tips of 50 nm radius were produced for the emission study.

The carbon nanotubes in this study were deposited using microwave plasma enhanced CVD operated at 1.5 kW. An n-type Si substrate was first deposited with 300 Å Fe and then nanotube growth was continued in the CVD reactor with 20 sccm CH_4 and 80 sccm H_2 at a pressure of 50 Torr and a substrate temperature of 900°C. The Fe catalytic layer is patterned to form a 50×50 array of 8 μm squares with 16 μm spacing. After 30 min of deposition, we observed multi-wall tubes of 10 μm in length and 20–50 nm in diameter with a random orientation (Fig. 1).

The growth of SiCN films has been described in detail elsewhere [13]. In short, an electron cyclotron resonance (ECR) plasma CVD reactor operating at a microwave power of 1200 W with a gas ratio of $CH_3NH_2:SiH_4:N_2:H_2 = 50:1:125:125$ and a silicon substrate temperature of 700°C was utilized to deposit nano-crystalline SiCN films of 300 nm thick on a silicon substrate. The typical stoichiometry of the SiCN films
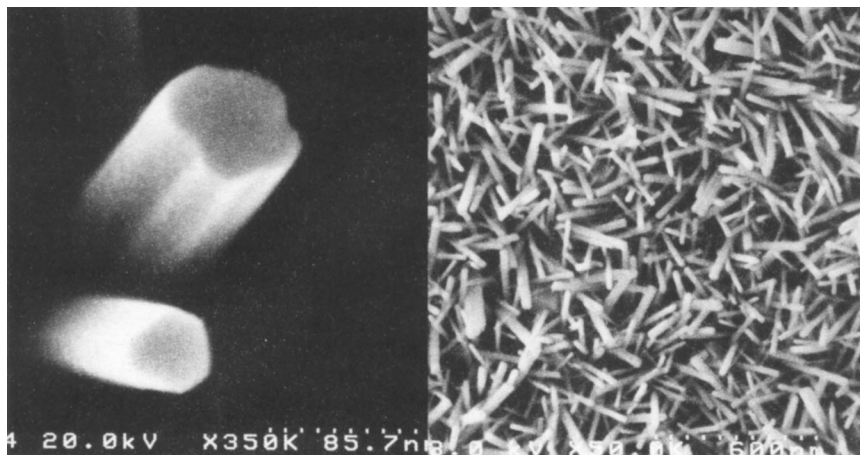

Fig. 2. Typical high-resolution SEM micrograph of SiCN nanorods.

thus deposited was $(Si;C)_3N_4$ with Si/C ranging from 1 to 2. The films thus deposited had a hexagonal structure with typical lattice constants of $a = 7.70$ Å, and $c = 5.78$ Å.

In addition to the crystalline films described above, SiCN exhibited another phase of reduced dimensionality. By using a proprietary buffer layer of 30 nm before regular MWPE-CVD, one-dimensional SiCN rods of 20–60 nm with an aspect ratio of 50 were deposited. A high-resolution SEM image of the SiCN nanorods is shown in Fig. 2, indicating well-faceted nanorods with a six-sided cross-section. The detailed growth mechanism and characteristics of the SiCN nanorods are not included in this paper and will be reported elsewhere [11].

2.2. Field emission measurement

The field emission characteristics were obtained using standard *I–V* measurement under a high vacuum with a base pressure of 2×10^{-7} Torr, as given in Fig. 3. A rectangular graphite electrode of 2×3 cm^2 was placed 30 μm above the sample. A Keithely multimeter was employed for sourcing the voltage and measuring the current. Precautions were taken to clean the sample before measurement in order to eliminate any dust particles on the surface that might have caused false signals. During the measurement, the voltage increase was adjusted to allow a detailed study of the *I–V* characteristics. The option to hold the voltage and record the emission current at a constant voltage makes possible, emission stability measurement, which is important for practical applications.

2.3. Other characterization

The morphology of the films was analyzed using a Hitachi scanning electron microscope (S-5000), which
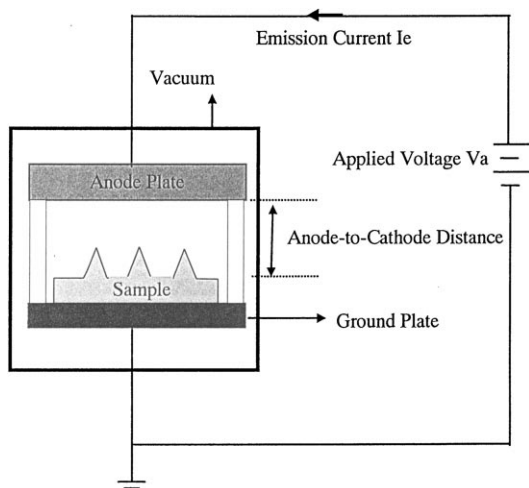

Fig. 3. Schematics of the set-up for field emission measurement.

is a high-resolution field emission SEM, allowing a magnification of up to 300 000. The composition of the sample was analyzed by a Perkin Elmer scanning Auger nanoprobe system (SAN760), which allows depth profile data to be acquired from an area as small as 500 Å. Further composition and chemical bonding information were determined by X-ray photoelectron spectroscopy (XPS) using a Perkin Elmer Phi 1600 ESCA system. MgKα radiation with an energy of 1253.6 eV was used as the source with a linewidth of 0.7 eV. Depth profiling with the XPS was performed by 4 kV Ar ion-beam bombardment of the sample.

3. Results and discussion

3.1. Emission from BAC silicon tips

Typical emission characteristics from the 50×50 BAC silicon tips are shown in Fig. 4. A turn-on field of 20 V/μm and an emission current of 120 μA at 36.7 V/μm were achieved. The F–N plot in the inset of Fig. 4 gave an effective barrier height of 0.017 eV, assuming a field enhancement factor of 31.6 from geometrical calculations. Note that the total current instead of current density is specified in this case due to the fact that it is an array of tips instead of a plain uniform film in our study. Therefore, it is meaningless to compare the current density as in the latter cases in this paper. In practical applications, the total current divided by the number of tips yielding the emission current per tip provides the most meaningful values.

3.2. Emission from carbon nanotubes

Typical emission characteristics of carbon nanotubes are shown in Fig. 5, in which a turn-on field strength of 10 V/μm and a maximum current of 3.8 mA at 16.7 V/μm were demonstrated. Multiple emission peaks were observed in Fig. 5, indicating emission site damage in the film and the subsequent appearance of newer emission sites at higher voltages, which is quite common in most carbon-nanotube samples. The phenomenon that several groups of emission sites coexist in a carbon-nanotube sample can be attributed to the different height of the nanotube, various diameters, and the different curvature or different types of tubes. Further studies are needed to determine the role of each factor on the emission at different stages. The F–N plot in the inset of Fig. 5 shows multiple emission groups, of which each individual group showed a linear relationship that follows the F–N equation.

Taking into account a total number of 2500 squares in each array and a 64 μm^2 area for each square, one obtains a current density of 2.6 A/cm^2 at 16.7 V/cm, which is far beyond the emission current density of

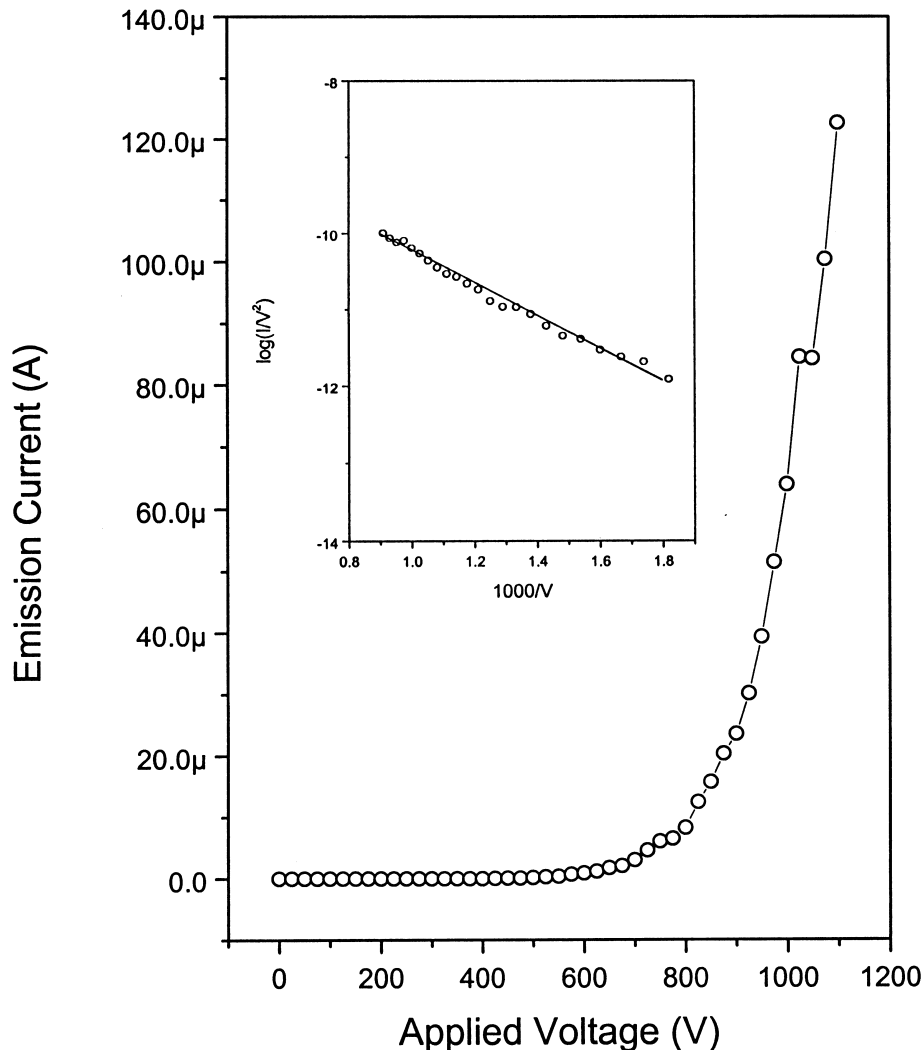Fig. 4. Field emission I–V curve and the corresponding F–N plot (inset) of 50 × 50 BAC silicon microtip arrays.

other materials at a comparable field. It still needs to be verified whether a larger-area carbon-nanotube sample will have the same performance as the array-type sample. None the less, the arrayed carbon nanotubes demonstrate a great potential for various electron sources applications including that for microwave devices.

3.3. Emission from SiCN films

The electron emissions of three SiCN films are shown in Fig. 6, in which a turn-on field of 13 V/μm and a maximum current density of 0.7 mA/cm² at 36.7 V/μm have been demonstrated. The current density is relatively small, compared with that of carbon nanotubes. However, the 0.7 mA/ cm²emission current density is several orders of magnitude higher than that of ordinary silicon or diamond films. The three sets of data from the top, middle, and bottom shown in Fig. 6 are taken

from three samples of composition ratios [C]:[Si]:[N] of 22:21:57, 13:32:55, and 0:41:59, respectively. It is quite clear that carbon incorporation into the film is essential for the field emission enhancement. Meanwhile, the origins of signal oscillation that occurs at a high applied field are still unclear and will be investigated further. The F–N plots in Fig. 6 show different slopes for samples of various composition, which can be attributed to the different barrier heights of the films.

3.4. Emission from SiCN nanorods

Fig. 7 shows the emission characteristics of a SiCN nanorod sample. Compared to that of SiCN films, a higher emission current of 1.5 mA/cm² at 35 V/μm with a turn-on field of 10 V/μm was observed. The enhancement in emission properties can be attributed to the geometric factor of the nanorod structure as well as the change in barrier height due to the variation in
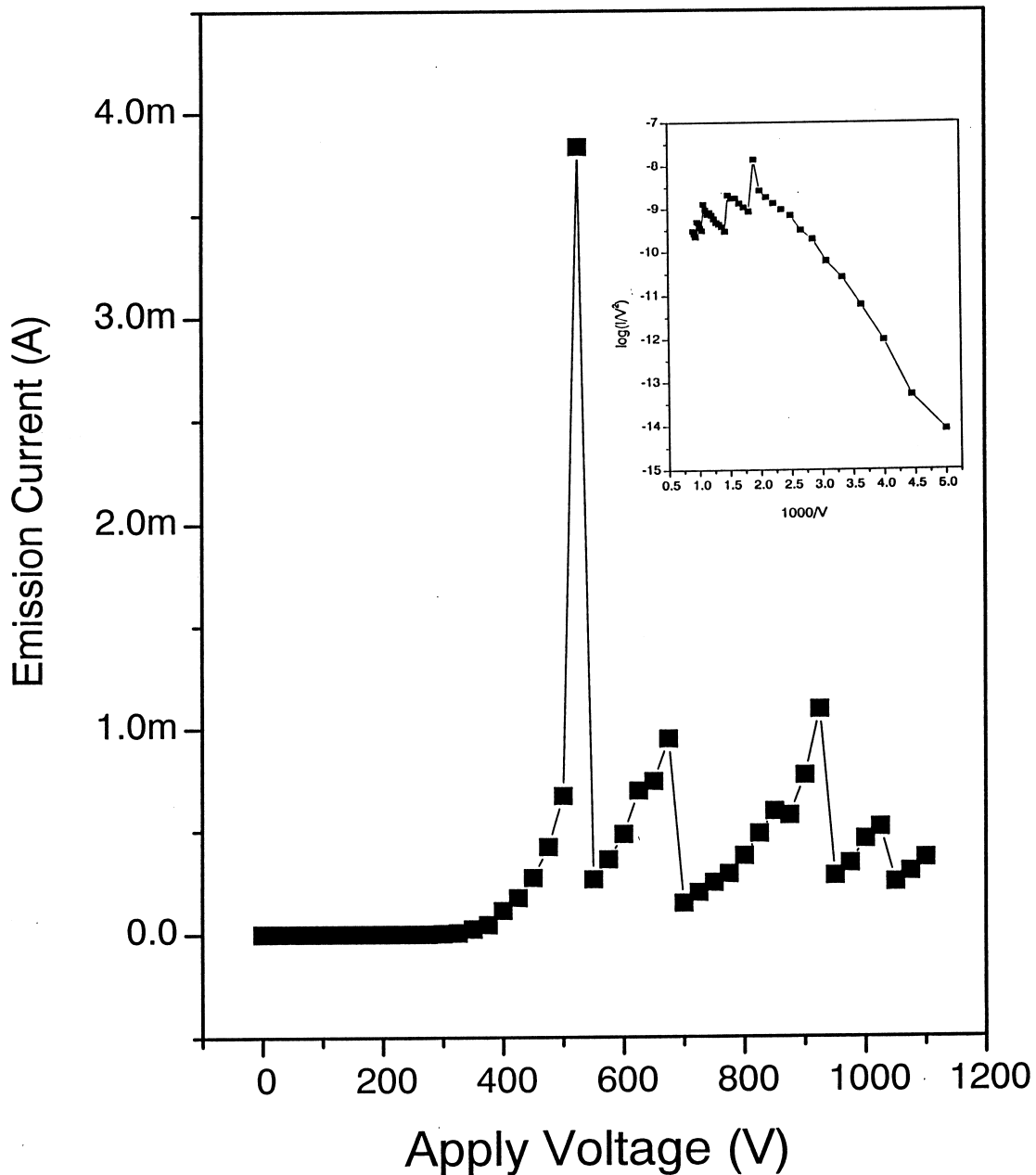
Fig. 5. Field emission *I–V* curve and the corresponding F–N plot (inset) of an array containing the 50 × 50 squares of carbon nanotubes.

composition/structure of the material. Remarkably, the F–N plot in the inset of Fig. 7 shows an excellent linear relationship over the entire range of applied field, indicating ideal field emission characteristics.

The Fowler–Nordheim description of the field emission can be expressed as

$$J = A \frac{F^2}{\phi} \exp\left(\frac{-B\phi^{3/2}}{F} \right), \tag{1}$$

where $A = 0.014$ and $B = 6.8 \times 10^9$ are constants. The units in the Fowler–Nordheim equation are: current

density, J (A/m^2), $F = \beta V/d$ with voltage, V (volts), distance, d (m), ϕ, the effective barrier height in (eV), and β the field enhancement factor that depends on the emitter geometry. Since there are only two parameters, β and ϕ, in this equation, a linear fit in the F–N plot allows us to derive the field enhancement factor as well as the effective barrier height of the emitter, which can provide an insight into the physics of the field emission. However, the current density in the Fowler–Nordheim equation is often not well defined due to the ambiguity in the emission area, which is difficult to determine especially for materials of an irregular surface morphol-
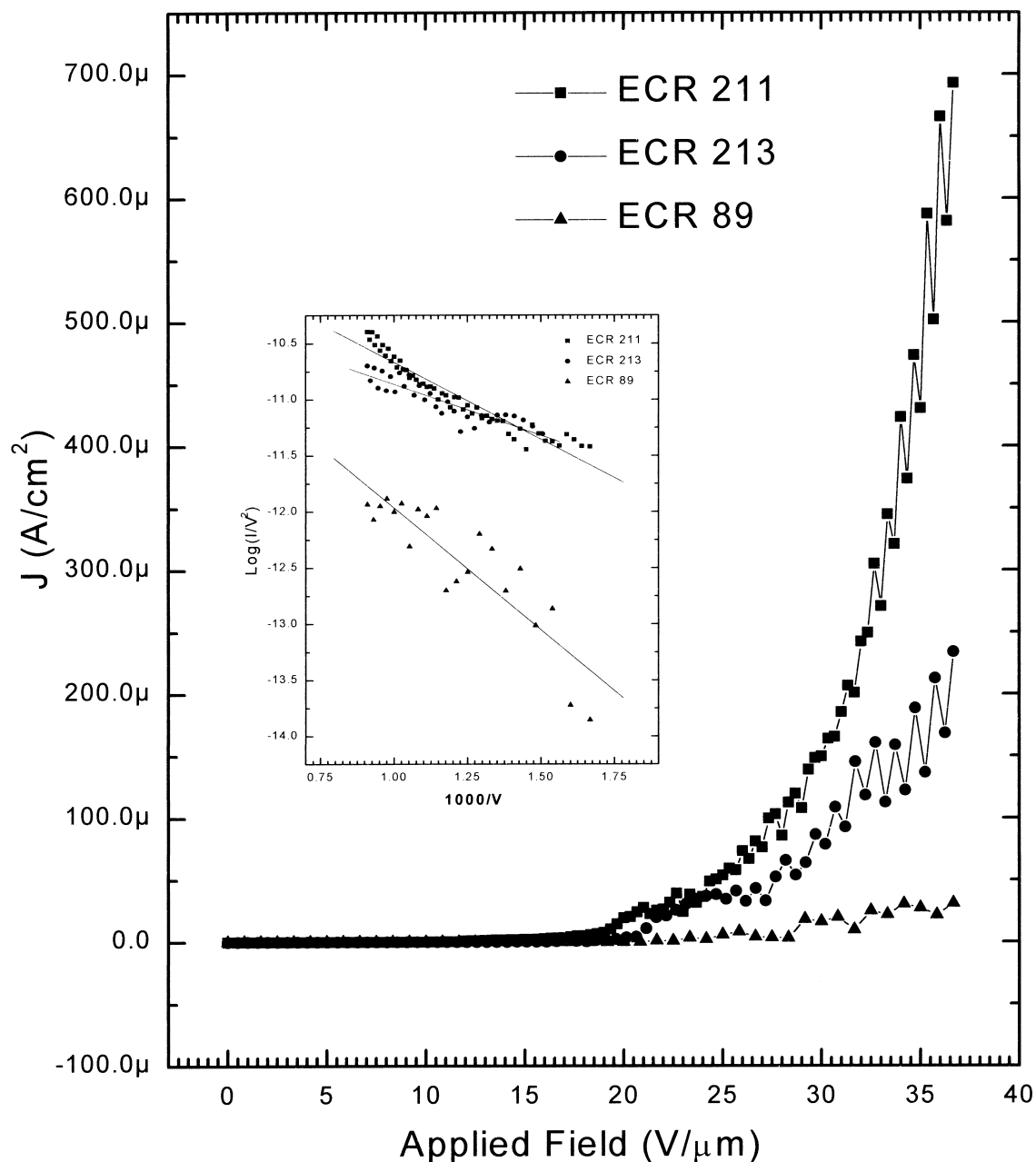
Fig. 6. Field emission *I–V* curve and the corresponding F–N plot (inset) of three SiCN films with composition ratios [C]:[Si]:[N] of 22:21:57(■), 13:32:55(●), and 0:41:59(▲).

ogy like nano-crystallites, nanotubes, and nanorods. Therefore, there are three unknown parameters, β, ϕ, and the emission area, in the Fowler–Nordheim equation instead of two parameters as mentioned earlier. Apparently, a linear fit in F–N plot only provides two parameters, slope and intersection, from which it is not possible to determine all the unknown parameters. Therefore, instead of providing the key parameters, β and ϕ, an F–N plot can only be used to exemplify the field emission characteristics.

3.5. Stability comparison of the carbon nanotubes and SiCN nanorods

While achieving the highest emission current at the lowest applied field is the goal in most field emission studies, the long-term stability of the emission is also an essential issue to be addressed. A comparison of the emission stability of a carbon-nanotube sample and a SiCN-nanorod sample is shown in Fig. 8. Although the carbon-nanotube sample showed a higher emission cur-
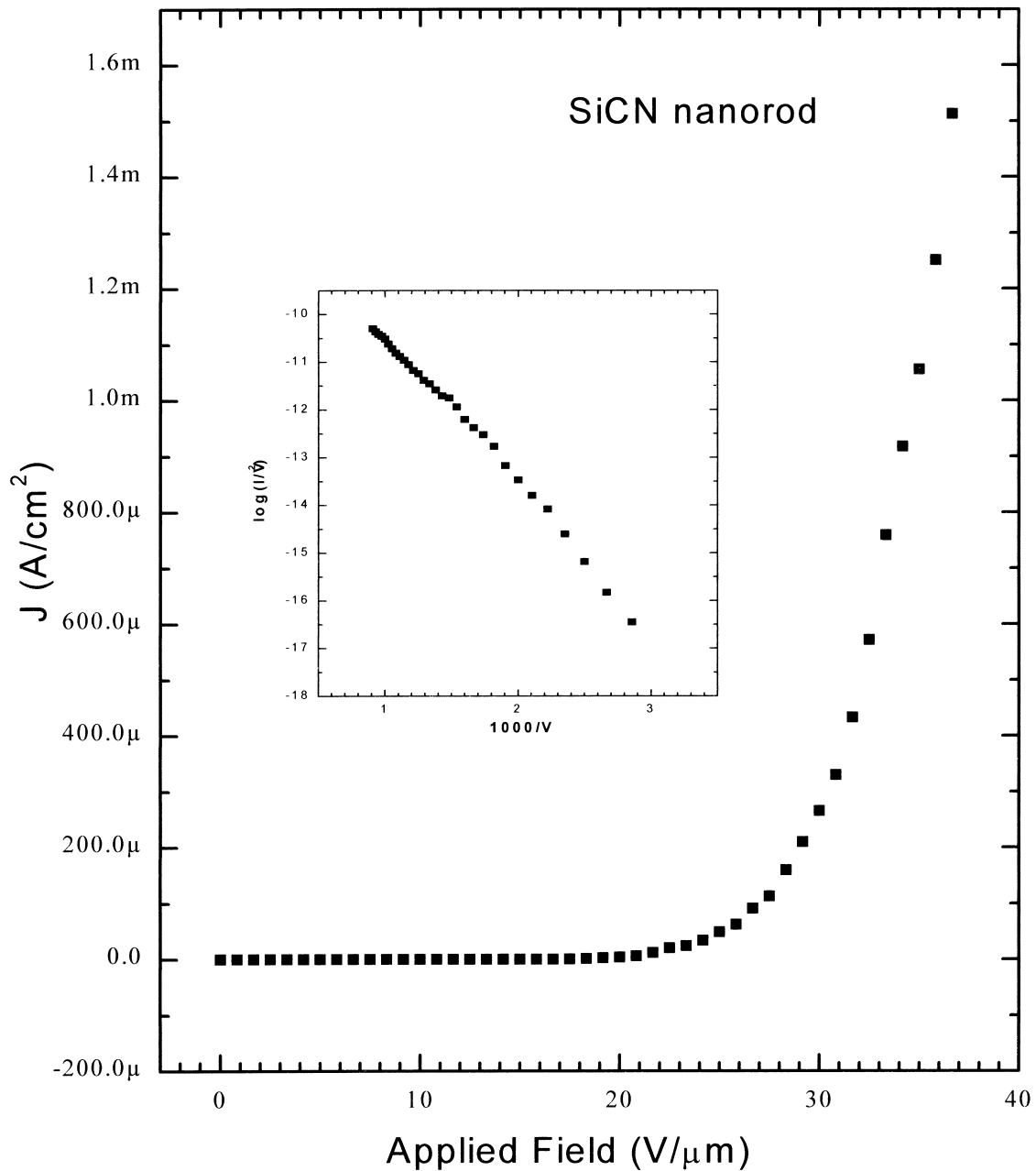
Fig. 7. Field emission *I–V* curve and the corresponding F–N plot (inset) of SiCN nanorods.

rent (3.8 mA for an array of 50×50 squares), the emission current decayed to 15% of the initial value after 1000 s of operation. In contrast, the SiCN nanorods showed a lower emission current (1.5 mA/cm^2), but the decay was much slower, about 50% decay after 1000 s of operation. It should be pointed out that the stability measurement has not been standardized so far. In our case, an operating condition near the maximum emission current is chosen for the test. The decay characteristics will be very different if we choose another test condition such as half the emission current. Therefore, it would

be wise to define the emission stability by the stressed emission at either specific current densities or at a specific applied field.

4. Conclusion

Among the four types of materials studied for electron field emission, carbon nanotubes deposited by MWPECVD demonstrated the highest emission current, which is several orders of magnitude higher than that
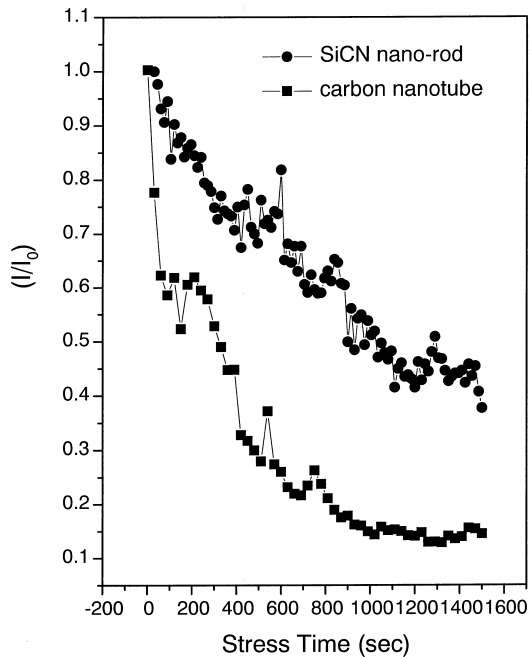
Fig. 8. Long-term stability of the field emission of SiCN nanorod (●) and carbon nanotubes (■).

of diamond films. However, SiCN films and nanorods showed a moderate emission current, which is comparable to most of the 'good' emitters. However, the stability of the emitters should be emphasized to meet the requirement of practical applications. Moreover, the issue of deriving an effective barrier height and the field enhancement factor in Fowler–Nordhiem equation is addressed. It is concluded that a definitive effective emission surface area is needed to solve the F–N equation completely and to obtain all the physical parameters.

References

[1] C. Wang, A. Garcia, D.C. Ingram, M.E. Kordesh, Electron. Lett. 27 (1991) 1459.
[2] M.W. Geis, N.N. Efremov, J.D. Woodhouse, M.D. McAleese, M. Marchywka, D.G. Socker, J.F. Hochedez, IEEE Electron Device Lett. 12 (1991) 456.
[3] M.W. Geis, J.C. Angus, Sci. Am. (1992) 84 October.
[4] W. Zhu, G.P. Kochanski, S. Jin, L. Seibles, J. Appl. Phys. 78 (1995) 2707.
[5] B.S. Satyanarayana, A. Hart, W.I. Milne, J. Robertson, Appl. Phys. Lett. 71 (1997) 1430.
[6] K. Okano, S. Koizumi, S. Ravi, P. Silva, G.A.J. Amaratunga, Nature 389 (1996) 140.
[7] L. Diederich, O.M. Kuttel, P. Aebi, L. Schlapbach, Diamond Relat. Mater. 8 (1999) 743.
[8] P.D. Kichambare, F.G. Tarntair, L.C. Chen, K.H. Chen, H.C. Cheng, J. Vac. Sci. Tech. (1999) (communication).
[9] L.C. Chen, T.R. Lu, C.T. Kuo, D.M. Bhusari, J.J. Wu, K.H. Chen, T.M. Chen, Appl. Phys. Lett. 72 (1998) 3449.
[10] L.C. Chen, C.Y. Yang, D.M. Bhusari, K.H. Chen, M.C. Lin, J.C. Lin, T.J. Chuang, Diamond Relat. Mater. 5 (1996) 514.
[11] K.H. Chen, J.J. Wu, S.L. Wei, C.Y. Wen, L.C. Chen, P.F. Kuo, Y.F. Chen, in: Handbook of Advance Electronic and Photonic Materials, H.S. Nalwa (Ed.). Academic Press, in press.
[12] T.W. Ebbesen, P.M. Ajayan, Nature 358 (1992) 220.
[13] K.H. Chen, J.J. Wu, C.Y. Wen, L.C. Chen, C.W. Fan, P.F. Kuo, Y.F. Chen, Thin Solid Films 355–356 (1999) 205.